

**Self-energy and fluctuation spectra in cuprates: Comparing optical and photoemission results**R. S. Markiewicz,<sup>1</sup> Tanmoy Das,<sup>1,2</sup> and A. Bansil<sup>1</sup><sup>1</sup>*Physics Department, Northeastern University, Boston, Massachusetts, 02115, USA*<sup>2</sup>*Theoretical Division, Los Alamos National Laboratory, Los Alamos, New Mexico, 87545, USA*

(Received 18 June 2010; revised manuscript received 25 June 2012; published 12 July 2012)

We compare efforts to extract self-energies and fluctuation spectra of the cuprates using optical and photoemission techniques. The fluctuations have contributions from both the coherent and incoherent parts of the band, which are spread over the full bare bandwidth of  $> 2$  eV. Many experimental studies concentrate on the coherent part of the band and hence miss higher-energy fluctuations. Our study establishes the universal presence of high-energy bosonic fluctuations across various spectroscopies as a key ingredient in the high-temperature superconducting cuprates.

DOI: [10.1103/PhysRevB.86.024511](https://doi.org/10.1103/PhysRevB.86.024511)

PACS number(s): 74.25.Gz, 74.20.-z, 74.72.-h, 78.20.-e

**I. INTRODUCTION**

A critical issue in unlocking the mechanism of superconductivity in the cuprates is determining the spectrum of bosonic (phononic or electronic) fluctuations that strongly interact with the electrons and that can drive a variety of instabilities and exotic physics. In particular, what is the energy scale of the relevant fluctuations: If high- $T_c$  superconductivity is produced by fluctuations at a low-energy scale comparable to the magnetic resonance mode,<sup>1</sup> then the bosons responsible for pairing, the so-called glue, could be phonons or magnetic excitations. If, on the other hand, higher-energy fluctuations ( $\sim J$ ,  $U$ , or charge transfer scales) play an important role,<sup>2-5</sup> a novel electronic mechanism would be clearly indicated.

Recently there have been a number of attempts to extract self-energies and fluctuation spectra of the cuprates from angle-resolved photoemission (ARPES), tunneling, and optical spectra. Most experimental probes find strong coupling to a low-energy boson:<sup>6-11</sup> often with significant isotope effect.<sup>12-14</sup> In addition, ARPES finds a high-energy kink (HEK) suggestive of significant coupling to electronic bosons in the 300–600 meV range.<sup>15-22</sup> These bosons are believed to be predominantly magnetic,<sup>23,24</sup> with charge bosons at higher energies up to the charge-transfer energy  $\sim 2$  eV. In contrast, recent attempts to extract the fluctuation spectra or the “optical glue”<sup>25</sup> functions from optical measurements<sup>6,7,9-11</sup> find little evidence for spectral weight above  $\sim 300$  meV, suggesting that high-energy scales are unimportant in the cuprates. However, these analyses are generally restricted to energies below  $\sim 1$  eV, thereby precluding the possibility of fluctuations at the  $\sim 2$  eV charge transfer energy scale (the  $U$  scale of the one-band Hubbard model).<sup>26</sup>

Several recent attempts at quasi-first-principles calculations of the optical spectra have found that the cuprate intraband optical spectrum extends up to  $\sim 2.5$  eV, with a residual charge transfer gap, associated with the incoherent part of the band, persisting well into the overdoped regime.<sup>27-30</sup> This suggests that optical glue studies should be extended into the higher-energy regime, to provide definitive answers about the role of charge transfer excitations in high- $T_c$  superconductivity. This is important since several optical studies<sup>11,31</sup> have found evidence that the onset of superconductivity affects spectral weight in an energy range extending beyond 1 eV.

In the present paper, we explore how the results of realistic self-energy calculations can be used to guide the analysis of the optical glue. We explore the role of anisotropy and clarify just what the glue function actually measures. We point out a simple correction to commonly used formulas for self-energy, which largely eliminates the problem of negative scattering rates. We find that an important contribution to the high-energy fluctuations has been “hiding in plain sight.” And we provide an example of an optical glue recovery which includes the high-energy contribution, and which bears a striking similarity to the calculated results. Our study thus resolves a puzzling discrepancy between optical versus other experiments related to the nature of bosonic fluctuations, and clearly demonstrates that experimental attempts to extract the optical glue need to probe a higher energy range to weigh in on the issue of a possible  $U$ -scale glue involved in the mechanism of high- $T_c$  superconductivity.

This paper is organized as follows. Section II A shows how including self-energy effects in optical calculations can provide insight into attempts to extract fluctuation, or “pairing glue” functions, from optical experiments. Section II B provides an example of extracting glue functions from real optical data. Section III describes numerical experiments to test the accuracy of the glue extraction, while Sec. IV compares the optical self-energy to ARPES-derived self-energies. Sections V and VI give a discussion and conclusions, respectively. Details of our self-energy calculations are presented in an Appendix.

**II. CALCULATING THE “GLUE” FUNCTION****A. General considerations**

We first briefly comment on how the optical “glue” is measured and what it really represents. One starts with the optical conductivity  $\sigma(\omega)$ , which can be calculated following Allen.<sup>32</sup> For a  $k$ -independent  $\Sigma$ :

$$\sigma(\omega) = \frac{i\omega_p^2}{4\pi\omega} \int_{-\infty}^{\infty} d\omega' \frac{n_F(\omega') - n_F(\omega' + \omega)}{\omega + \Sigma^*(\omega') - \Sigma(\omega' + \omega)}, \quad (1)$$

where  $n_F$  is the Fermi function. In optical glue studies, an “optical self-energy” function is derived from the experimental optical conductivity  $\sigma$  by assuming it to be of an extended

Drude form<sup>33,34</sup>

$$\sigma(\omega) = \frac{i\omega_p^2}{4\pi} \frac{1}{\omega - 2\Sigma_{\text{op}}(\omega)}, \quad (2)$$

where  $\omega_p = \sqrt{4\pi n e^2/m}$  is the plasma frequency,  $n$  the carrier density, and  $e, m$  are the electronic charge and mass, respectively. This can also be written in terms of a frequency-dependent scattering time  $\tau(\omega)$  and effective mass  $m^*(\omega)$  as

$$2\Sigma_{\text{op}}(\omega) = \omega \left( 1 - \frac{m^*}{m} \right) - \frac{i}{\tau}. \quad (3)$$

An important question is how is  $\Sigma_{\text{op}}$  related to the self-energy function  $\Sigma$ ? Two approaches are commonly employed, which we call Method I, which simply assumes

$$\Sigma_{\text{op}} = \Sigma, \quad (4)$$

and Method II:<sup>35–38</sup>

$$\Sigma_{\text{op}} = \frac{\int_0^\omega \Sigma(\omega') d\omega'}{\omega}. \quad (5)$$

We test these schemes in Sec. III, by comparing self-energies extracted from calculated optical spectra with the input self-energies, calculated using a GW model<sup>39</sup> appropriate for the cuprates. We find similar results for both methods: They can approximately reproduce  $\Sigma''$  at energies below  $\sim 1$  eV, but both methods have problems in the pseudogap regime.

In the GW method, the self-energy is calculated as the convolution of the Green's function  $G$  and an interaction  $W$  which is  $U^2$  times a susceptibility, which represents the spectrum of electronic bosonic modes (see the Appendix for details). For cuprates with  $d$ -wave pairing, the true pairing glue is given by the  $d$ -wave average of this  $q$ -dependent function. In contrast, the optical spectra are measured at  $q = 0$  and provide no information on this anisotropy. Hence optical experiments can only measure an average  $\bar{W}$ , which we nevertheless denote as  $\alpha^2 F$ . Below we show that  $\alpha^2 F$  approximately represents the  $q$ -averaged susceptibility:

$$\alpha^2 F(\omega) = U^2 [\bar{\chi}_c''(\omega) + 3\bar{\chi}_s''(\omega)]/2, \quad (6)$$

with  $U$  the Hubbard  $U$ ,  $\chi''$  the imaginary part of  $\chi$ ,  $\chi_c$  ( $\chi_s$ ) the charge (spin) susceptibility, and we neglect the distinction between  $\alpha^2 F$  and  $\alpha_u^2 F$ , where the latter is a transport Eliashberg function. Also  $\bar{\chi}_i(\omega) = \int a^2 d^2q \chi_i(\mathbf{q}, \omega)/(2\pi)^2$ ,  $i = s, c$ . Within RPA,

$$\chi_s = \chi_0/(1 - U\chi_0), \quad (7)$$

$$\chi_c = \chi_0/\epsilon, \quad (8)$$

where  $\chi_0$  is the bare susceptibility as calculated in the local-density approximation (LDA), and the dielectric constant can be written as  $\epsilon = \epsilon_0 + U\chi_0$  with  $\epsilon_0 \sim 4.8$ , a background dielectric constant. Thus optical measurements determine the  $q$ -averaged susceptibility as a function of energy. This can be compared to susceptibilities measured in other spectroscopies, such as ARPES, to determine the spectra of the bosons which strongly couple to electrons, but cannot directly provide information on how well these bosons contribute to  $d$ -wave superconductivity.

When the susceptibility is replaced by its  $q$  average, the formula for the self-energy can be simplified (see the

Appendix). At  $T = 0$ , for  $\omega > 0$ , it becomes

$$\Sigma''(\omega) = - \int_0^\omega \alpha^2 F(\Omega) \tilde{N}(\omega - \Omega) d\Omega, \quad (9)$$

where  $\tilde{N}(\omega) = [N(\omega) + N(-\omega)]/2N_{\text{av}}$  is the electron-hole-averaged density of states (DOS), and  $N_{\text{av}}$  is the average of the DOS over the energy range of interest, chosen to make  $\tilde{N}$  dimensionless. Then for Method II,

$$\Sigma''_{\text{op}}(\omega) = \int_0^\omega \frac{d\Omega}{\omega} \alpha^2 F(\Omega) n_{\text{eh}}(\omega - \Omega), \quad (10)$$

where

$$n_{\text{eh}}(\omega) = \int_0^\omega d\omega' \tilde{N}(\omega'). \quad (11)$$

We note that in many previous inversion schemes the DOS is approximated by a constant. In this case Eq. (9) becomes<sup>40</sup>

$$\alpha^2 F_0(\omega) = - \frac{\partial \Sigma''_{\text{op}}(\omega)}{\partial \omega}. \quad (12)$$

We use the subscript 0 on  $\alpha^2 F$  to denote that it is assumed a constant DOS. According to Eq. (12) the glue function can become negative unless  $|\Sigma''_{\text{op}}|$  is a monotonically increasing function of  $\omega$ .<sup>41</sup> We find that  $\alpha^2 F$  and  $\alpha^2 F_0$  can display very different energy dependencies as can be seen by comparing Figures 4(a) and 4(b) below. A similar problem arises with Method II.<sup>35</sup> Many groups use a finite-temperature version of this result.<sup>11,42</sup> From Eq. (10), it follows that  $-\partial \Sigma''_{\text{op}}/\partial \omega$  must be  $> 0$ , as for Eq. (12), and

$$\alpha^2 F_1(\omega) = - \frac{\partial}{\partial \omega} [\omega^2 \alpha^2 F_0(\omega)], \quad (13)$$

where  $\alpha^2 F_1$  is the glue function corresponding to Eq. (10). While this works for phonon contributions to the self-energy, this substitution is not appropriate over a 2–3 eV energy range. We find that  $\Sigma''$  cannot be monotonic over the full bandwidth, and that may be why previous analyses often had problems with negative  $\alpha^2 F$ , or why they are restricted to fairly low energies. In contrast, these problems do not arise with Eqs. (9) and (10).

The question remains, what is the appropriate DOS? This has two aspects. First, since the optical self-energy  $\Sigma''_{\text{op}}$  involves the sum of the electron and hole self-energies, one should use the average of the electron and hole DOS,  $\tilde{N}$  in Eq. (9). But which DOS? In the GW approach, one could consider using either the bare  $N_0$  or the fully dressed DOS  $N$ . The use of  $N$  is prohibitively expensive, since to calculate it requires knowledge of the glue function, which we are trying to extract. On the other hand,  $N_0$  can be directly calculated from the LDA dispersion and should work progressively better with overdisping, as correlation effects weaken. For simplicity, in the present analysis we use  $N_0$ . This approximation should have no effect on the qualitative features we are describing.

## B. Application to Bi2212

Figure 1(a) compares the measured<sup>43</sup> optical conductivity of near-optimally doped  $\text{Bi}_2\text{Sr}_2\text{CaCu}_2\text{O}_{8+\delta}$  (Bi2212) (red dotted line)<sup>44,45</sup> and  $\text{La}_{2-x}\text{Sr}_x\text{CuO}_4$  (LSCO)<sup>46</sup> (green solid line) with calculated<sup>27</sup> (blue dashed line) conductivities for

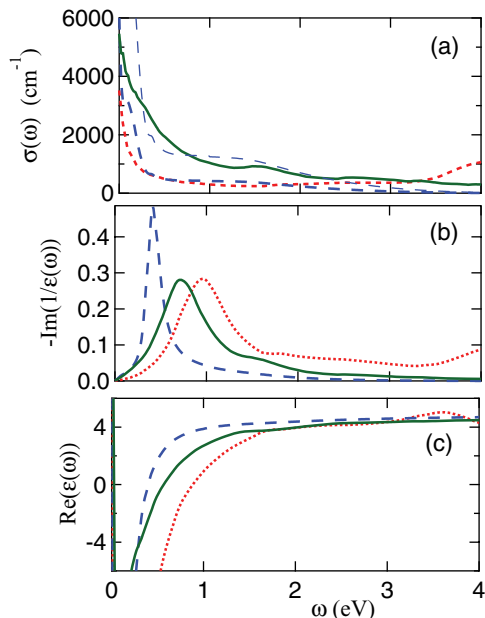


FIG. 1. (Color online) (a) Optical conductivity of optimally doped Bi2212 ( $a$  axis)<sup>43</sup> (red short-dashed line) and  $x = 0.15$  LSCO<sup>46</sup> (green solid line) compared with theory for LSCO<sup>27</sup> (blue dashed line; expanded  $\times 3$ : thin blue dashed line). (b) Corresponding loss function,  $-\text{Im}(1/\epsilon(\omega))$ . (c) Dielectric constant  $\epsilon$ .

LSCO. The theoretical conductivity consists of a Drude term associated with the coherent part of the electronic band plus an effective interband term associated with the incoherent spectral weight, a residue of the upper and lower magnetic bands. While the theory underestimates the incoherent spectral weight (a known shortcoming of the QP-GW model),<sup>47,48</sup> it does capture an enhanced conductivity near 1.5 eV, associated with this residual charge transfer band.<sup>27</sup> Given the conductivity, the corresponding dielectric constant and inverse dielectric constants can readily be calculated. These are shown in Figs. 1(b) and 1(c) for LSCO, to be compared to the experimental results for Bi2212. The good agreement strongly suggests that all features in the spectrum up to  $\sim 2.5$  eV are characteristic features of the cuprate plane, and are well described by a single-band Hubbard model.<sup>49</sup> Note that the electronic susceptibility should be nonzero over the same frequency window as the loss function, so both charge and spin contributions to the glue function should remain finite up to  $\sim 2.5$  eV, which is approximately the bare (LDA) electronic bandwidth.

Given the optical spectrum, we can extract the glue function over the full bandwidth. Figure 2(a) plots the optical self-energy of Bi2212 (solid blue line) extracted from the data in Fig. 1<sup>43</sup> using Eq. (2). For simplicity, we calculated  $\Sigma_{\text{op}}$  using the full optical spectrum, but the features above  $\sim 2.5$  eV are probably due to interband transitions, and hence should be disregarded. In the low-energy limit, the self-energy is in reasonable agreement with earlier work<sup>50</sup> (blue triangles), which neglected the DOS factor. Shown also are model self-energies calculated from Eq. (9) or Eq. (10), using the glue function plotted in Fig. 2(b) as a red dashed line and the DOS of Fig. 2(c). For the present illustrative purposes, we use

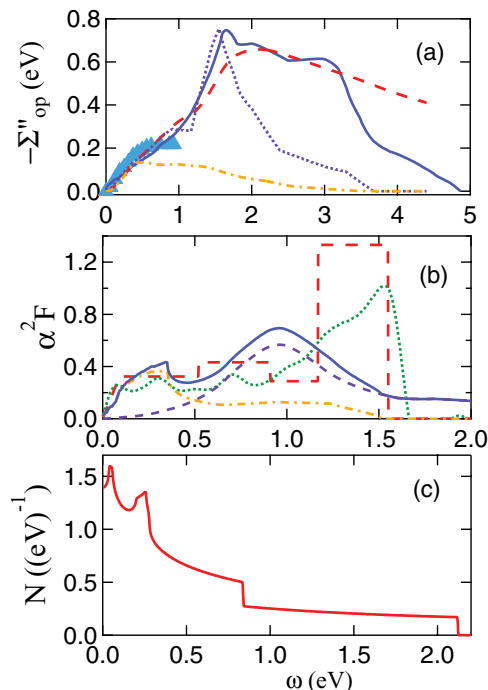


FIG. 2. (Color online) (a) Optical self-energy extracted from the experimental data<sup>43</sup> of Fig. 1 (dark blue solid line), compared with calculated self-energies using Eq. (10) (red dashed line) or Eq. (9) (violet dotted line) and the corresponding glue function from frame (b) (red dashed line). Also shown is the low-energy measured self-energy<sup>50</sup> (blue triangles) from Fig. 6. (b) Glue functions used in frame (a). Green dotted line is glue function calculated from Eq. (12). These are compared with calculated glue functions, including the calculated spin  $\alpha^2 F_s$  of Fig. 4(b) (orange dot-dashed line), the charge glue function [Eq. (14)] with  $U_{c,\text{eff}} = 2\text{eV}$  (violet dashed line), and their sum (blue solid line). (c) Electron-hole-averaged bare DOS for Bi2212.

$T = 0$  expressions to analyze the spectrum, even though the experiments were done at room temperature.

In our model calculation, we represent the glue function by a simple histogram, red-dashed line in Fig. 2(b). We find a very good fit to the data using Method II, red dashed line in Fig. 2(a). Using the same glue function, the self-energy calculated by Method I [violet dotted line in Fig. 2(a)] fits the data well below 1.5 eV, but falls off too rapidly at higher energies. An improved fit would therefore require additional weight in the glue function at even higher energies, which seems less likely. Remarkably, the green dashed line in Fig. 2(b) shows that the glue function can also be approximately found from Eq. (12), if we neglect the negative glue function contributions at higher energy.

According to Eq. (6), the glue function should be calculable in terms of the spin and charge susceptibilities. In a previous publication<sup>48</sup> we showed that the charge susceptibility that enters the self-energy should be the same as in the loss function plotted in Fig. 1(b). However, from Fig. 1(b), it can be seen that the present model does not well reproduce the experimental loss function, perhaps because the Hubbard model does not describe the charge susceptibility of Eq. (8) well, and longer-range Coulomb interactions need to be included.<sup>23,47,51</sup> We can avoid this difficulty by directly comparing two experimental measures of the loss function, taking the charge contribution

to the glue function as

$$\alpha^2 F_c(\omega) = -\frac{U_{c,\text{eff}}}{2} \text{Im} \left[ \frac{1}{\epsilon(\omega)} \right], \quad (14)$$

where  $U_{c,\text{eff}}$  is a phenomenological charge vertex, and  $\epsilon$  is the measured dielectric constant. In Fig. 2(d), we compare the extracted glue function with the calculated spin susceptibility of Fig. 4(b) (orange dot-dashed line) [the corresponding self-energy is plotted in Fig. 2(a), orange dot-dashed line]. There is satisfactory agreement up to 0.5 eV, but the experimental glue function reveals excess weight in the charge-transfer regime above 1 eV. There should be an extra contribution due to charge fluctuations, which we plot in Fig. 2(b), using the experimental loss function from Fig. 1(b) in Eq. (14). Figure 2(b) shows that the combination of spin and charge glue functions qualitatively reproduces the glue function extracted directly from the optical spectrum, including a significant contribution near 1 eV. Differences above 1 eV may be due to limitations in extracting the true  $\Sigma$  from  $\Sigma_{\text{op}}$ , as discussed in the following section. We note that the contribution of the loss function to the optical glue has not been previously recognized.

### III. TESTING OPTICAL INVERSION SCHEMES

#### A. Connecting $\Sigma$ and $\alpha^2 F$

Having a realistic scheme for calculating optical spectra allows us to test how well glue functions can be extracted, by inverting calculated data and comparing the inverted with the input susceptibilities. Here we briefly describe the results of several tests we have carried out. We first note that while the  $q$  dependence of  $\chi''$  is important, the self-energy is a convolution over  $\chi$  and the Green's function, and we find that its momentum dependence is relatively weak in the overdoped regime. This is important, since when the self-energy has a significant momentum dependence, the Kubo formula for conductivity includes significant vertex corrections,<sup>52</sup> which to our knowledge have not been included in any inversion scheme. Fortunately, the weak momentum dependence of the self-energy that we find suggests that a self-energy extracted from optical studies could still be fairly representative.

Since optical techniques can only find a momentum-averaged glue function, in Fig. 3 we address the issue of the extent to which the average glue function can reproduce the self-energy.<sup>53-55</sup> We denote this momentum-averaged glue

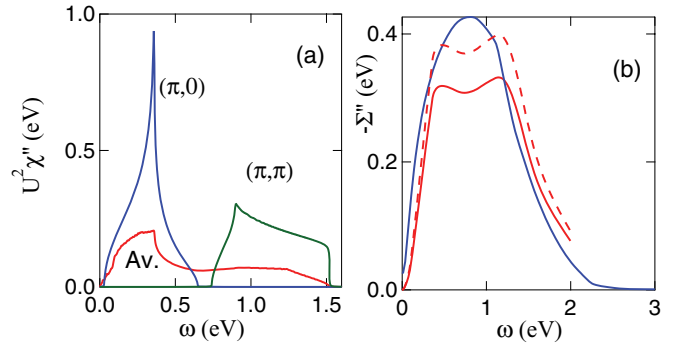


FIG. 3. (Color online) (a) Imaginary susceptibility  $\chi''_s$  at  $T = 0$  plotted along two directions in  $k$  space,  $(\pi,0)$  (blue line) and  $(\pi,\pi)$  (green line), along with the value averaged over all  $k$  (red line). (b) Resulting imaginary self-energy  $\Sigma''$ , comparing the exact anisotropic calculation (blue line) with the present isotropic approximation (red line), and a scaled isotropic calculation multiplied by 1.2 (dashed red line).

function as  $\alpha^2 F(\omega)$ . To avoid tensor complications we limit our analysis to the overdoped normal state spectra and analyze only the RPA magnetic susceptibility  $\chi_s = \chi_0/(1 - U\chi_0)$ , with bare susceptibility  $\chi_0$  and  $U$  being the Hubbard  $U$ . In Fig. 3(a) the average  $\bar{\chi}''_s$  is compared to individual  $\chi''_s$  peaks, demonstrating that there is significant anisotropy in  $\chi''_s$ . The weight in  $\bar{\chi}''_s$  extends to energies  $\sim 1.5$  eV, in good agreement with early optical determinations.<sup>31</sup> Figure 3(b) compares the calculated  $\Sigma''$  using either the correct expression, Eq. (A3) below (blue line), or the angle-averaged Eq. (9) value (red line). It can be seen that averaging before integrating underestimates the magnitude of  $\Sigma''$ , by about 20% (dashed line), but approximately reproduces the shape of  $\Sigma''$ . Hence we estimate that the average glue function extracted from optical spectra should have the correct frequency dependence, but could be overestimated by  $\sim 20\%$  in intensity.

Once the self-energy is known, we can invert it to try to recover the susceptibility. Here as a test case we take a derivative of  $\Sigma$  [Eq. (9)] and fit the  $-\partial\Sigma''/\partial\omega$  data using a bar graph representation for  $\bar{\chi}''$ .<sup>10</sup> We illustrate the calculation with only two bars, which works reasonably well, but the generalization to many bars is straightforward. Thus, if  $\alpha^2 F(\omega) = \alpha^2 F_1$  for  $\omega < \omega_1$ ,  $\alpha^2 F_2$  for  $\omega_1 \leq \omega < \omega_2$ , and 0 for  $\omega \geq \omega_2$ , then

$$-\frac{1}{2} \frac{\partial \Sigma''(\omega)}{\partial \omega} = \begin{cases} \alpha^2 F_1 N(\omega) & \omega < \omega_1 \\ \alpha^2 F_1 [N(\omega) - N(\omega - \omega_1)] + \alpha^2 F_2 N(\omega - \omega_1) & \omega_1 \leq \omega < \omega_2 \\ \alpha^2 F_1 [N(\omega) - N(\omega - \omega_1)] + \alpha^2 F_2 [N(\omega - \omega_1) - N(\omega - \omega_2)] & \omega \geq \omega_2. \end{cases} \quad (15)$$

Figure 4(a) shows a fit using this procedure, with  $-\partial\Sigma''/\partial\omega$  taken from the correct self-energy [blue curve in Fig. 3(b)]. For a simple two-step glue function, the fit is remarkably good, and could be further improved by adding more steps. Figure 4(b) shows that the resulting  $\alpha^2 F$  is a reasonable reproduction of the input form. Exact agreement is not expected, since the calculated  $\alpha^2 F$  is the scaled average used to generate the approximate self-energy [red dashed curve in

Fig. 3(b)], whereas the extracted glue function is based in the exact self-energy (calculated with anisotropic susceptibility). The similarity of the two glue functions provides additional evidence that the angle-averaged formula captures the essential physics. The two peaks in  $\alpha^2 F$  have a simple interpretation, the lower peak, below 0.5 eV, represents the fluctuation spectrum of the coherent part of the band, while the peak near 1 eV represents the fluctuations responsible for opening

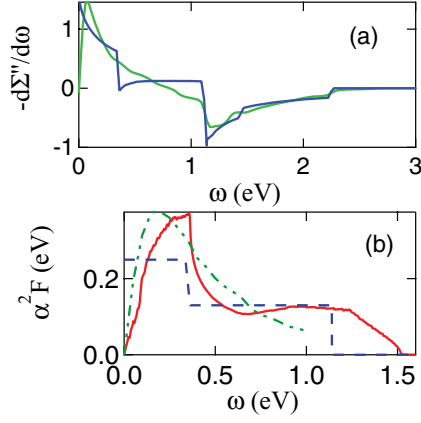


FIG. 4. (Color online) (a)  $-\partial\Sigma'/\partial\omega$  (green line) compared with fit based on Eq. (15) (blue line). (b) Glue functions, comparing the calculated  $\alpha^2F$  (blue dashed line) with the input function from Fig. 4(a) (red line), and with an earlier optical glue function<sup>8</sup> (green dot-dot-dashed line).

the charge-transfer gap at lower doping. A glimpse at Fig. 3(a) reveals that these are heavily concentrated near  $(\pi, \pi)$ .

Most previous analyses of the optical glue are consistent with the coherent part of Fig. 4(b), displaying a peak near 0.3 eV. For instance, the dot-dot-dashed line in Fig. 4(b) shows the “continuum” glue function extracted from optical experiments in Ref. 8. However, they also find a sharper peak at low energies, below  $\sim 0.1$  eV, not reproduced by the present calculation. We suggest that this peak may be associated either with phonons or with superconducting or pseudogap effects (e.g., related to the magnetic resonance peak), none of which are included in the present normal state analysis. We note that when superconductivity is included, our susceptibility calculations can reproduce many features of the magnetic resonance phenomenon.<sup>56</sup>

### B. The weak link: From $\Sigma_{\text{op}}$ to $\Sigma$

Finally, we test how well the true self-energy can be extracted from  $\Sigma_{\text{op}}$  in Eq. (2). First, we expand Eq. (1) in the small  $\omega$  limit, in which case  $n_F(\omega') - n_F(\omega' + \omega) \simeq \omega\delta(\omega')$  at  $T = 0$ , while  $\omega + \Sigma^*(\omega') - \Sigma(\omega' + \omega) = \omega[1 - \partial\Sigma'(\omega)/\partial\omega] - 2i\Sigma''(\omega)$ , so that Eq. (1) becomes

$$\sigma(\omega) = \frac{i\omega_p^2}{4\pi} \frac{1}{\omega - \omega[\partial\Sigma'(\omega)/\partial\omega] - 2i\Sigma''(\omega)}. \quad (16)$$

Comparing Eq. (2) and Eq. (16),

$$\Sigma'_{\text{op}}(\omega) = [\partial\Sigma'(\omega)/\partial\omega]\omega/2, \quad (17)$$

$$\Sigma''_{\text{op}}(\omega) = \Sigma''(\omega). \quad (18)$$

In the special case where  $\Sigma'$  is quadratic in  $\omega$ ,  $\Sigma_{\text{op}} = \Sigma$ , the Method I result. However, we generally find  $\Sigma' \sim \omega$  at low frequencies, so  $\Sigma'_{\text{op}}$  and  $\Sigma'$  differ by a factor of 2, and  $\Sigma_{\text{op}}$  does not satisfy the Kramers-Kronig relation.

Despite this limitation,  $\Sigma_{\text{op}}$  can be used to extract the quasiparticle self-energy, at least in the low-energy regime at not-too-low doping. Figure 5 compares the quasiparticle self-energy  $\Sigma$  of NCCO to  $\Sigma_{\text{op}}$  calculated by first computing

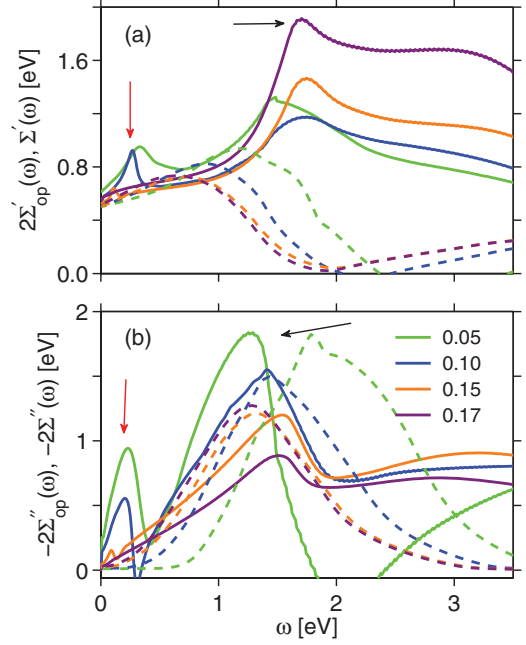


FIG. 5. (Color online) The computed values of the optical self-energies (solid lines) are compared with the corresponding quasiparticle self-energy (dashed lines of same color) for a series of dopings for NCCO.<sup>55,57</sup> Both results agree well in the low-energy, high-doping region.

the optical conductivity,<sup>57</sup> and then extracting  $\Sigma_{\text{op}}$  via Eq. (2). The optical conductivity is calculated from a standard linear response theory in the presence of an antiferromagnetic pseudogap and the quasiparticle self-energy  $\Sigma$  corrections. In accord with experimental results in NCCO, the optical spectra show two distinct features, a mid-infrared feature originating from the pseudogap order and the high-energy Mott gap feature associated with the magnon scattering peak in  $\Sigma''$ .<sup>57</sup>

Figure 5 shows that Eqs. (17) and (18) hold in the low-energy region for the paramagnetic phase. However, for the underdoped samples ( $x = 0.05, 0.10, 0.15$ )  $\Sigma_{\text{op}}$  shows an additional kink at low energies coming from the pseudogap feature, not present in the quasiparticle self-energy. (The calculated quasiparticle self-energy includes the antiferromagnetic pseudogap, but this arises in the off-diagonal term of a  $2 \times 2$  tensor and is not captured in the scalar approximation  $\Sigma_{\text{op}}$ .) Thus, near optimal doping optical studies should be able to determine  $\Sigma''$  in the range up to  $\sim 1$  eV, but the calculation breaks down in the underdoped regime. For work at higher energies a more sophisticated approach is needed. One possibility would be to use model self-energies to reproduce the experimental spectra. We have illustrated the comparison for Method I, but very similar results are found for Method II.

## IV. MAGNITUDE OF SELF-ENERGY IN ARPES AND OPTICAL STUDIES

While the energy dependence of the self-energy is readily extracted from optical or ARPES experiments, we find that there are subtle issues in normalizing the spectra. ARPES probes the one-particle self-energy, with full momentum

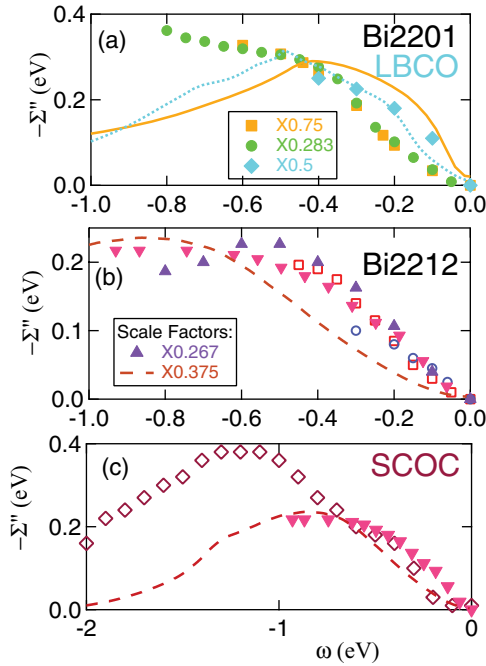


FIG. 6. (Color online) Imaginary self-energy  $\Sigma''$  at  $T = 0$  vs energy  $\omega$ , comparing experimental and theoretical results derived by several techniques. In all cases an impurity contribution was approximately removed by subtracting off  $\Sigma''(0)$ . Experimental points are ARPES data from: (a) LSCO (blue diamonds, Ref. 18); Bi2201 (gold squares, Ref. 17; green circles, Ref. 19); (b) Bi2212 (violet triangles, Ref. 18; open red squares, Ref. 20; open blue circles, Ref. 21), and (c)  $\text{Ca}_2\text{CuO}_2\text{Cl}_2$  (CCOC) (open red-brown diamonds, Ref. 22). Included in (b) and (c) are optical data from Bi2212 (inverted red triangles, Ref. 50) (taken at  $T = 130\text{K} > T_c$  to avoid complications associated with superconductivity). Theoretical curves are from LSCO (light blue dotted line), Ref. 27; Bi2201 (gold line), Ref. 23; Bi2212 (red dashed line), Ref. 24. Note that the magnitudes of several data sets have been rescaled.

dependence, but only for the filled states.<sup>58–62</sup> Figure 6 shows measured<sup>17–22</sup> and calculated values<sup>55,63</sup> of the imaginary self-energy  $\Sigma''$  as a function of excitation energy  $\omega$ . The data represent a number of different cuprates at several dopings, but in all cases  $\Sigma''(\omega)$  has a similar shape. There is a clear but relatively weak material dependence, in good agreement with calculations.

However, the experiments fail to find a consistent *magnitude* of  $\Sigma''$ , with values varying by a factor of four, sometimes [as in the case of Bi2201; Fig. 6(a)] on virtually the same material measured by two different groups. This is because  $\Sigma''$  is not measured directly. Instead, data were acquired by measuring the momentum-space width  $\Delta k$  of a spectral peak and then multiplying by the “bare Fermi velocity,”  $v_{F0}$ . Unfortunately, the bare velocity is not a measured quantity, and a variety of techniques have been utilized for estimating the value. The largest  $\Sigma$  are found by assuming the bare and dressed dispersions do not cross, hence drawing the bare dispersion as a straight line that either lies below the ARPES dispersion or touches it at some high energy. This assumption is equivalent, via Kramers-Kronig, to assuming that  $\Sigma''$  is monotonic in energy. Neither of these features is consistent

with theory (see Ref. 23 and Fig. 6), and moreover, most experiments find that the ARPES linewidth narrows again at higher energies; i.e.,  $\Sigma''$  should have a peak in the region of the HEK. Note that for a band of finite width it can be shown analytically that  $\Sigma'' \rightarrow 0$  as  $\omega \rightarrow \infty$ .

Using a smaller  $v_{F0}$  brings the result into better agreement with theory. The best choice for the bare dispersion is probably the first-principles LDA calculation.<sup>64,65</sup> However, it is also possible for experiments to find a too small value of  $v_{F0}$ . This is because in Bi2212 the self-energy is large enough that the peak in  $\Sigma''$  (the high-energy kink) splits the dispersion into low- and high-energy branches, with a pseudogap in between. ARPES experiments find the coherent band in Bi2212 is renormalized by a factor of  $Z = 0.5$  with coherent spectral weight extending to a band bottom at the  $\Gamma$  point near  $-0.5$  eV,<sup>66,67</sup> whereas incoherent spectral weight extends  $\sim > 1$  eV below the Fermi level. If only this coherent branch is considered in extracting the self-energy, the resulting  $\Sigma''$  will be underestimated by the same factor  $Z = 0.5$ , consistent with the smallest values found in Fig. 6.

The Dresden group<sup>21</sup> attempted to extract both self-energy and bare dispersion, treating the  $\Gamma \rightarrow (\pi/2, \pi/2)$  (nodal) bare dispersion as a parabola, and adjusting the magnitude of the dispersion until the real and imaginary self-energies satisfied Kramers-Kronig relations. The resulting bare band can be parametrized by the energy of the band bottom at  $\Gamma$ ,  $E_0(\Gamma) = -0.9$  eV for Bi-2212 at optimal doping. In contrast, the corresponding LDA result is  $-1.55$  eV. This suggests either that LDA is not a good model for the bare bands or that the extracted self-energies are too small by approximately the ratio of the  $E_0(\Gamma)$ , 0.6. This is indeed close to the difference seen between their experiment and theory in Fig. 6.

We note that our calculations involve only electronic bosons, whereas experiments suggest that phonons may play a role in the temperature dependent broadening of the optical spectra, even in the undoped insulators.<sup>68</sup> This could explain some of the differences between calculated and experimental self-energies.

Figure 6(a) and 6(b) also displays the optically derived  $\Sigma'' = -1/2\tau$  from Ref. 50. We see that its energy dependence is in good agreement with theory, but its magnitude is smaller than theory by a factor of 2, consistent with some ARPES evaluations. In optical studies one can encounter a similar problem to those found in photoemission. If  $m^*(\omega) = m_1^* + m_2^*(\omega)$ , then we can rewrite

$$\sigma(\omega) = \frac{i\omega_p^{*2}}{4\pi} \frac{1}{\omega(1 + m_2^{**}/m) + i/\tau^*(\omega)}, \quad (19)$$

where  $\omega_p^{*2} = Z\omega_p^2$ ,  $m_2^{**} = Zm_2^*$ , and  $1/\tau^* = Z/\tau$ , with  $Z = m/m_1^*$ . We note that if  $\omega_p^*$  is used in Eq. (2), then the frequency dependence of the extracted  $\Sigma''$  is correctly given by the measured  $\sigma$ , but its magnitude is too small by the factor  $Z$ .

## V. DISCUSSION

The present study finds that both low- and high-energy fluctuations couple strongly to electronic excitations in the cuprates. This has important implications for the origin of superconductivity in these materials, and in particular is

suggestive of two-component  $\alpha^2 F$  models, with a strong peak at low frequencies and a weak (electronic) peak at very high frequencies.<sup>69,70</sup> In Ref. 4, we showed that in a hole-overdoped cuprate  $x = 0.3$ , the glue functions below and above 0.3 eV made comparable contributions to the superconducting gap. This is consistent with the predictions of Refs. 2 and 3 but is contradicted by another study which finds that low-energy fluctuations in the vicinity of the magnetic resonance peak can by themselves produce a 100 K superconductor.<sup>71</sup> The difference would seem to be that the latter study explored only the role of fluctuations near the resonance, whereas our full susceptibility calculation found an important role of ferromagnetic pairbreaking fluctuations, widely expected to be limiting  $T_c$  on the overdoped side.<sup>72,73</sup> As Cohen and Anderson<sup>74</sup> have noted, a key impediment to finding high  $T_c$  superconductors is the emergence of competing phases.

## VI. CONCLUSIONS

In conclusion, our study provides a number of insights into attempts to derive self-energies and glue functions from experimental studies of the cuprates. We find a surprising variability in the magnitude of self-energy reported in different studies. We have identified possible sources and recommend use of first-principles dispersions in the analyses to minimize the problem. With respect to specifically optical studies, we find that the self-energy is relatively momentum independent, so these studies should be useful for extracting momentum-averaged fluctuation spectra. A possible weak link is relating the optical spectrum to an underlying self-energy, as the usual  $\Sigma_{\text{op}}$  is found to deviate from the true  $\Sigma$  at energies above  $\sim 1$  eV.

Most importantly, we have shown that in the overdoped regime the optical spectra of the cuprates should be described in a single-band model for energies below  $\sim 2.5$  eV. When this is done, the resulting fluctuation spectrum or glue function displays substantial spectral weight in the high-energy region extending to  $\sim 1.5$  eV. Our study thus finds additional high-energy bosonic fluctuations in the optical spectra and reconciles a puzzling discrepancy in this regard involving optical and other spectroscopies. In the conventional terminology of optical studies, these contributions should also be considered as part of the optical “glue” function.

Of course, from optical studies there is no way of determining which of the observed fluctuations promote d-wave superconductivity, which play no role in superconductivity, and which are actually pair breaking. Nevertheless, we must abandon the common perception that optical studies “prove” that only low-frequency bosonic fluctuations are important for high- $T_c$  superconductivity, particularly when those studies are restricted to energies below  $\sim 1$  eV.

## ACKNOWLEDGMENTS

This work is supported by the U.S.D.O.E contract DE-FG02-07ER46352 and benefited from the allocation of supercomputer time at NERSC and Northeastern University’s Advanced Scientific Computation Center (ASCC). This work was begun while R.S.M. was on sabbatical at the University

of Rome, partially funded by the Marie Curie Grant PIIF-GA-2008-220790 SOQCS. R.S.M. acknowledges stimulating conversations with M. Grilli.

## APPENDIX: MODEL SELF-ENERGY FOR CUPRATES

A recent series of calculations has led to a reassessment of the strength of correlations in cuprates. It has been found that, within a single-band Hubbard model,  $U \leq 8t$  is too small to satisfy the Brinkman-Rice criterion for a Mott transition, and the magnetic phase in the cuprates is closer to a conventional (Slater-type) antiferromagnet.<sup>75,76</sup> Here  $U$  is the Hubbard  $U$ -parameter and  $t$  is the nearest neighbor hopping. With doping, spectral weight is transferred from the “upper Hubbard band” to low energies too rapidly to be consistent with a  $U = \infty$  Hubbard or a  $t$ - $J$  model.<sup>77</sup> In contrast, intermediate coupling models can describe this anomalous spectral weight transfer,<sup>28,78</sup> and more generally provide a good description of angle-resolved photoemission spectroscopy (ARPES) and optical spectra over a wide doping and energy range.<sup>23,27,29,30</sup> In these models, a self-energy is derived either from dynamic mean-field theory calculations or from a modified GW procedure. Here we describe the modified GW self-energy calculation.

In the metallic phase at high doping, the quasiparticle-GW (QP-GW) self-energy  $\Sigma$  is given by a convolution over the green function  $G$  and the interaction  $W \sim U^2 \chi$  as<sup>24,79–82</sup>

$$\begin{aligned} \tilde{\Sigma}(\mathbf{k}, \sigma, i\omega_n) = & \frac{1}{2} U^2 Z \sum_{\mathbf{q}, \sigma'} \eta_{\sigma, \sigma'} \int_0^\infty \frac{d\omega_p}{2\pi} \tilde{G}(\mathbf{k} + \mathbf{q}, \sigma', i\omega_n, \omega_p) \\ & \times \Gamma(\mathbf{k}, \mathbf{q}, i\omega_n, \omega_p) \text{Im}[\tilde{\chi}_{\text{RPA}}^{\sigma\sigma'}(\mathbf{q}, \omega_p)]. \end{aligned} \quad (\text{A1})$$

where  $\sigma$  is the spin index and  $\eta_{\sigma, \sigma'}$  is 3 for the spin and 1 for the charge modes. Extensions to the antiferromagnetic and/or superconducting phases are described in the references. In the QP-GW scheme,  $\Sigma$  is calculated self-consistently, with  $G$  and  $W$  calculated from an approximate self-energy  $\Sigma'_0(\omega) = (1 - Z^{-1})\omega$ , where the renormalization factor  $Z$  is adjusted self-consistently to match the coherent (low-energy) part of the self-energy.<sup>23,48,81</sup> The vertex correction  $\Gamma$  in Eq. (A1) is taken as (Ward’s identity)  $\Gamma = 1/Z$ . We take the dispersions directly from LDA calculations ( $\xi_{\mathbf{k}}$ ), accurately fitted by a one-band tight-binding model,<sup>83</sup> without any adjustment of the resulting parameters.<sup>84–86</sup> In the overdoped regime a value for the screened Hubbard  $U = 1$  eV is used.<sup>27</sup> In Eq. (A1) we use the RPA magnetic and charge susceptibilities. Since the  $k$  dependence of  $\Sigma$  is weak,<sup>23</sup> we further simplify the calculation by assuming a  $k$ -independent  $\Sigma$ , which we calculate at a representative point  $k = (\pi/2, \pi/2)$ .

When the correct susceptibility is replaced by a  $k$ -averaged version, the formula for the self-energy simplifies. The GW self-energy can be written:

$$\begin{aligned} \Sigma(\mathbf{q}, \omega) = & -\frac{3}{2} U^2 \sum_{\mathbf{k}} \int_{-\infty}^\infty \chi''(\mathbf{k}, \Omega) d\Omega \int_{-\infty}^\infty A(\mathbf{k} + \mathbf{q}, \epsilon) d\epsilon \\ & \times \left[ \frac{n_B(\Omega) + n_F(\epsilon)}{\omega + \Omega - \epsilon} + \frac{n_B(\Omega) + 1 - n_F(\epsilon)}{\omega - \Omega - \epsilon} \right], \end{aligned} \quad (\text{A2})$$

where  $A(\mathbf{k}, \epsilon)$  is the electronic spectral function,  $n_F$  [ $n_B$ ] is the Fermi [Bose] function, and  $\chi''$  is the imaginary part of an

appropriate susceptibility.<sup>23,87</sup> Then

$$\Sigma''(\mathbf{q}, \omega) = -\frac{3}{2}U^2 \sum_{\mathbf{k}} \int_{-\infty}^{\infty} \chi''(\mathbf{k}, \Omega) d\Omega \{A(\mathbf{k} + \mathbf{q}, \omega + \Omega)[n_B(\Omega) + n_F(\omega + \Omega)] + A(\mathbf{k} + \mathbf{q}, \omega - \Omega)[n_B(\Omega) + 1 - n_F(\omega - \Omega)]\}. \quad (\text{A3})$$

When  $\chi''$  is replaced by  $\bar{\chi}''$  in Eq. (A3), the  $\mathbf{k}$  sum reduces to  $\sum_{\mathbf{k}} A(\mathbf{k}, \epsilon) = N(\epsilon)$  and Eq. (A3) becomes<sup>88,89</sup>

$$\Sigma''(\omega) = -\frac{1}{2} \int_{-\infty}^{\infty} \frac{\alpha^2 F(\Omega)}{N_{\text{av}}} d\Omega \left\{ N(\omega + \Omega) \left[ \coth\left(\frac{\Omega}{2T}\right) - \tanh\left(\frac{\Omega + \omega}{2T}\right) \right] + N(\omega - \Omega) \left[ \coth\left(\frac{\Omega}{2T}\right) - \tanh\left(\frac{\Omega - \omega}{2T}\right) \right] \right\}. \quad (\text{A4})$$

At  $T = 0$  and  $\omega > 0$ , this becomes Eq. (9), while for  $\omega < 0$ , the only changes are that the upper limit of the integral is  $|\omega|$  and the argument of  $N$  is  $\Omega - |\omega|$  which is  $< 0$ .

- 
- <sup>1</sup>H. Woo, P. Dai, S. M. Hayden, H. A. Mook, T. Dahm, D. J. Scalapino, T. G. Perring, and F. Dogan, *Nat. Phys.* **2**, 600 (2006).  
<sup>2</sup>P. W. Anderson, *Science* **316**, 1705 (2007).  
<sup>3</sup>T. A. Maier, D. Poilblanc, and D. J. Scalapino, *Phys. Rev. Lett.* **100**, 237001 (2008).  
<sup>4</sup>R. S. Markiewicz and A. Bansil, *Phys. Rev. B* **78**, 134513 (2008).  
<sup>5</sup>V. J. Emery, *Phys. Rev. Lett.* **58**, 2794 (1987); V. J. Emery and G. Reiter, *Phys. Rev. B* **38**, 4547 (1988).  
<sup>6</sup>E. Schachinger and J. P. Carbotte, *Phys. Rev. B* **62**, 9054 (2000).  
<sup>7</sup>S. V. Dordevic, C. C. Homes, J. J. Tu, T. Valla, M. Strongin, P. D. Johnson, G. D. Gu, and D. N. Basov, *Phys. Rev. B* **71**, 104529 (2005).  
<sup>8</sup>P. Cásek, C. Bernhard, J. Humlíček, and D. Munzar, *Phys. Rev. B* **72**, 134526 (2005).  
<sup>9</sup>M. R. Norman and A. V. Chubukov, *Phys. Rev. B* **73**, 140501 (2006).  
<sup>10</sup>E. van Heumen, E. Muhlethaler, A. B. Kuzmenko, H. Eisaki, W. Meevasana, M. Greven, and D. van der Marel, *Phys. Rev. B* **79**, 184512 (2009).  
<sup>11</sup>C. Giannetti, F. Cilento, S. Dal Conte, G. Coslovich, G. Ferrini, H. Molegraaf, M. Raichle, R. Liang, H. Eisaki, M. Greven, A. Damascelli, D. van der Marel, and F. Parmigiani, *Nat. Comm.* **2**, 353 (2011).  
<sup>12</sup>Jinho Lee, K. Fujita, K. McElroy, J. A. Slezak, M. Wang, Y. Aiura, H. Bando, M. Ishikado, T. Masui, J.-X. Zhu, A. V. Balatsky, H. Eisaki, S. Uchida, and J. C. Davis, *Nature (London)* **442**, 546 (2006).  
<sup>13</sup>G.-H. Gweon, T. Sasagawa, S. Y. Zhou, J. Graf, H. Takagi, D.-H. Lee, and A. Lanzara, *Nature (London)* **430**, 187 (2004).  
<sup>14</sup>H. Iwasawa, J. F. Douglas, K. Sato, T. Masui, Y. Yoshida, Z. Sun, H. Eisaki, H. Bando, A. Ino, M. Arita, K. Shimada, H. Namatame, M. Taniguchi, S. Tajima, S. Uchida, T. Saitoh, D. S. Dessau, and Y. Aiura, *Phys. Rev. Lett.* **101**, 157005 (2008); K. Sato, H. Iwasawa, N. C. Plumb, T. Masui, Y. Yoshida, H. Eisaki, H. Bando, A. Ino, M. Arita, K. Shimada, H. Namatame, M. Taniguchi, S. Tajima, Y. Nishihara, D. S. Dessau, and Y. Aiura, *Phys. Rev. B* **80**, 212501 (2009).  
<sup>15</sup>F. Ronning, K. M. Shen, N. P. Armitage, A. Damascelli, D. H. Lu, Z.-X. Shen, L. L. Miller, and C. Kim, *Phys. Rev. B* **71**, 094518 (2005).  
<sup>16</sup>J. Graf, G.-H. Gweon, K. McElroy, S. Y. Zhou, C. Jozwiak, E. Rotenberg, A. Bill, T. Sasagawa, H. Eisaki, S. Uchida, H. Takagi, D.-H. Lee, and A. Lanzara, *Phys. Rev. Lett.* **98**, 067004 (2007).  
<sup>17</sup>W. Meevasana, X. J. Zhou, S. Sahrakorpi, W. S. Lee, W. L. Yang, K. Tanaka, N. Mannella, T. Yoshida, D. H. Lu, Y. L. Chen, R. H. He, Hsin Lin, S. Komiya, Y. Ando, F. Zhou, W. X. Ti, J. W. Xiong, Z. X. Zhao, T. Sasagawa, T. Kakeshita, K. Fujita, S. Uchida, H. Eisaki, A. Fujimori, Z. Hussain, R. S. Markiewicz, A. Bansil, N. Nagaosa, J. Zaanen, T. P. Devereaux, and Z.-X. Shen, *Phys. Rev. B* **75**, 174506 (2007).  
<sup>18</sup>T. Valla, T. E. Kidd, W.-G. Yin, G. D. Gu, P. D. Johnson, Z.-H. Pan, and A. V. Fedorov, *Phys. Rev. Lett.* **98**, 167003 (2007).  
<sup>19</sup>B. P. Xie, K. Yang, D. W. Shen, J. F. Zhao, H. W. Ou, J. Weil, S. Y. Gu, M. Arita, S. Qiao, H. Namatame, M. Taniguchi, N. Kaneko, H. Eisaki, K. D. Tsuei, C. M. Cheng, I. Vobornik, J. Fujii, G. Rossi, Z. Q. Yang, and D. L. Feng, *Phys. Rev. Lett.* **98**, 147001 (2007).  
<sup>20</sup>J. M. Bok, J. H. Yun, H.-Y. Choi, W. Zhang, X. J. Zhou, and C. M. Varma, *Phys. Rev. B* **81**, 174516 (2010).  
<sup>21</sup>A. A. Kordyuk, S. V. Borisenko, V. B. Zabolotnyy, J. Geck, M. Knupfer, J. Fink, B. Büchner, C. T. Lin, B. Keimer, H. Berger, A. V. Pan, S. Komiya, and Y. Ando, *Phys. Rev. Lett.* **97**, 017002 (2006).  
<sup>22</sup>C. Kim, S. R. Park, C. S. Leem, D. J. Song, H. U. Jin, H.-D. Kim, F. Ronning, and C. Kim, *Phys. Rev. B* **76**, 104505 (2007).  
<sup>23</sup>R. S. Markiewicz, S. Sahrakorpi, and A. Bansil, *Phys. Rev. B* **76**, 174514 (2007).  
<sup>24</sup>Susmita Basak, Tanmoy Das, Hsin Lin, J. Nieminen, M. Lindroos, R. S. Markiewicz, and A. Bansil, *Phys. Rev. B* **80**, 214520 (2009).  
<sup>25</sup>Notably, optical techniques cannot access the full  $\alpha^2 F(\mathbf{q}, \omega)$  needed for the symmetry-averaged  $d$ -wave glue; see D. J. Scalapino, E. Loh Jr., and J. E. Hirsch, *Phys. Rev. B* **34**, 8190 (1986); **35**, 6694 (1987) and Ref. 4.  
<sup>26</sup>For example, Ref. 11 presents optical spectra for Bi2212 extending to  $\sim 6$  eV, with a peak associated with the residual charge-transfer gap identified near 2.72 eV. While features below this energy are argued not to involve  $d$ - $d$  transitions, the spectrum is arbitrarily divided into an “intragap” part below 1.25 eV and an “interband” part at higher energies, and only the former is assumed to contribute to the glue function.



- <sup>27</sup>Tanmoy Das, R. S. Markiewicz, and A. Bansil, [arXiv:0807.4257](#); *Phys. Rev. B* **81**, 174504 (2010).
- <sup>28</sup>A. Comanac, L. de Medici, M. Capone, and A. J. Millis, *Nature Phys.* **4**, 287 (2008); L. de' Medici, X. Wang, M. Capone, and A. J. Millis, *Phys. Rev. B* **80**, 054501 (2009).
- <sup>29</sup>N. Lin, E. Gull, and A. J. Millis, *Phys. Rev. B* **82**, 045104 (2010), and references therein.
- <sup>30</sup>C. Weber, K. Haule, and G. Kotliar, *Nat. Phys.* **6**, 574 (2010).
- <sup>31</sup>M. J. Holcomb, J. P. Collman, and W. A. Little, *Phys. Rev. Lett.* **73**, 2360 (1994); H. J. A. Molegraaf, C. Presura, D. van der Marel, P. H. Kes, and M. Li, *Science* **295**, 2239 (2002).
- <sup>32</sup>P. B. Allen, [arXiv:cond-mat/0407777v1](#).
- <sup>33</sup>J. Hwang, T. Timusk, and G. D. Gu, *Nature (London)* **427**, 714 (2004).
- <sup>34</sup>J. Hwang, E. J. Nicol, T. Timusk, A. Knigavko, and J. P. Carbotte, *Phys. Rev. Lett.* **98**, 207002 (2007).
- <sup>35</sup>P. B. Allen, *Phys. Rev. B* **3**, 305 (1971).
- <sup>36</sup>F. Marsiglio, T. Startseva, and J. P. Carbotte, *Phys. Lett. A* **245**, 172 (1998); F. Marsiglio, *J. Supercond.* **12**, 163 (1999).
- <sup>37</sup>S. V. Shulga, *Material Science, Fundamental Properties and Future Electronic Applications of High-Tc Superconductors* (Kluwer Academic Publishers, Dordrecht, 2001), pp. 323–360.
- <sup>38</sup>J. Hwang, E. J. Nicol, T. Timusk, A. Knigavko, and J. P. Carbotte, *Phys. Rev. Lett.* **98**, 207002 (2007).
- <sup>39</sup>L. Hedin, *J. Phys.: Condens. Matter* **11**, R489 (1999).
- <sup>40</sup>This formula was generalized to finite temperatures by J. Hwang, T. Timusk, E. Schachinger, and J. P. Carbotte, *Phys. Rev. B* **75**, 144508 (2007). Notably, however, they still assume a constant density of states, and hence overlook the correction discussed here.
- <sup>41</sup>A similar problem arises when the spectrum has a gap; see Ref. 7.
- <sup>42</sup>E. G. Maksimov, *Phys. Usp.* **43**, 965 (2000).
- <sup>43</sup>M. A. Quijada, D. B. Tanner, R. J. Kelley, M. Onellion, H. Berger, and G. Margaritondo, *Phys. Rev. B* **60**, 14917 (1999).
- <sup>44</sup>This agreement justifies the assumed background subtraction in Ref. 27 and further suggests an interpretation of this background in terms of interband transitions to a  $d_{z^2}$ -like band, which is believed to be much closer to the Fermi level in LSCO than in other cuprates.<sup>45</sup>
- <sup>45</sup>H. Sakakibara, H. Usui, K. Kuroki, R. Arita, and H. Aoki, [arXiv:1003.1770](#).
- <sup>46</sup>S. Uchida, T. Ido, H. Takagi, T. Arima, Y. Tokura, and S. Tajima, *Phys. Rev. B* **43**, 7942 (1991).
- <sup>47</sup>We comment briefly on the deviation between theory and experiment in Fig. 1. First, we note that this was part of a comprehensive fit over the full doping range in Ref. 27, and no effort was made to adjust the parameters here. Second, we note that the problem is an underestimate of the strength of the residual charge transfer band, as shown by the thin blue dashed line in Fig. 1(a). This weakness leads to the fast falloff of  $\epsilon$  at higher frequencies [Fig. 1(c)]. Since the zero crossing of  $\epsilon$  fixes the plasmon peak, this leads to the peak in (b) being too sharp and at too low an energy. There are three possible sources of discrepancy. First, it could be that some of the parameters used in Ref. 27 have a weak doping dependence, which was neglected. Second, the QP-GW method is an approximation, which is designed to accurately capture the coherent part of the self-energy, but at the cost of underestimating the high-energy incoherent part of the self-energy. Third, this calculation approximated the dielectric constant in the Hubbard model as  $1 + U\chi$ , whereas we know that including long-range Coulomb interactions is important for the high-energy effects of the charge susceptibility.<sup>48</sup>
- <sup>48</sup>R. S. Markiewicz and A. Bansil, *Phys. Rev. B* **75**, 020508 (2007).
- <sup>49</sup>The feature in Bi2212 above 3.5 eV was suggested to be related to BiO-layer interband transitions,<sup>43</sup> and we confirm that it is not present in the one-band Hubbard model.
- <sup>50</sup>D. van der Marel, H. J. A. Molegraaf, J. Zaanen, Z. Nussinov, F. Carbone, A. Damascelli, H. Eisaki, M. Greven, P. H. Kes, and M. Li, *Nature (London)* **425**, 271 (2003).
- <sup>51</sup>R. S. Markiewicz, M. Z. Hasan, and A. Bansil, *Phys. Rev. B* **77**, 094518 (2008).
- <sup>52</sup>J. Chaloupka and D. Munzar, *Phys. Ref. B* **76**, 214502 (2007).
- <sup>53</sup>In these calculations, we work near optimal hole doping using parameters appropriate for NCCO, but most cuprates have similar susceptibilities.<sup>54</sup>
- <sup>54</sup>R. S. Markiewicz, J. Lorenzana, G. Seibold, and A. Bansil, *Phys. Rev. B* **81**, 014509 (2010).
- <sup>55</sup>Since the momentum dependence of  $\Sigma$  is weak, we take the result for  $q = (\pi/2, \pi/2)$  as representative.
- <sup>56</sup>T. Das, R. S. Markiewicz, and A. Bansil, *Phys. Rev. B* **85**, 144526 (2012); A. Bansil, Susmita Basak, Tanmoy Das, Hsin Lin, M. Lindroos, J. Nieminen, Ipo Suominen, and R. S. Markiewicz, *J. Phys. Chem. Solids* **71**, 341 (2011).
- <sup>57</sup>Tanmoy Das, R. S. Markiewicz and A. Bansil, *Phys. Rev. B* **81**, 184515 (2010).
- <sup>58</sup>We are not taking into account matrix element effects, which in general can be important in ARPES,<sup>59</sup> STM,<sup>60</sup> and other highly resolved spectroscopies.<sup>61,62</sup>
- <sup>59</sup>S. Sahrakorpi, M. Lindroos, R. S. Markiewicz, and A. Bansil, *Phys. Rev. Lett.* **95**, 157601 (2005); J. C. Campuzano, L. C. Smedskjaer, R. Benedek, G. Jennings, and A. Bansil, *Phys. Rev. B* **43**, 2788 (1991); A. Bansil, M. Lindroos, S. Sahrakorpi, and R. S. Markiewicz, *ibid.* **71**, 012503 (2005).
- <sup>60</sup>J. Nieminen, H. Lin, R. S. Markiewicz, and A. Bansil, *Phys. Rev. Lett.* **102**, 037001 (2009).
- <sup>61</sup>R. S. Markiewicz and A. Bansil, *Phys. Rev. Lett.* **96**, 107005 (2006); S. Huotari, K. Hamalainen, S. Manninen, S. Kaprzyk, A. Bansil, W. Caliebe, T. Buslaps, V. Honkimaki, and P. Suortti, *Phys. Rev. B* **62**, 7956 (2000); P. E. Mijnders and A. Bansil, *ibid.* **13**, 2381 (1976).
- <sup>62</sup>P. E. Mijnders, A. C. Kruseman, A. van Veen, H. Schut, and A. Bansil, *J. Physics: Condens. Matter* **10**, 10383 (1998); J. Mader, S. Berko, H. Krakauer, and A. Bansil, *Phys. Rev. Lett.* **37**, 1232 (1976); L. C. Smedskjaer, A. Bansil, U. Welp, Y. Fang, and K. G. Bailey, *Physica C* **192**, 259 (1992).
- <sup>63</sup>We calculate the self-energy due to magnetic fluctuations only, since these dominate within  $\sim 1$  eV of the Fermi level.
- <sup>64</sup>Care must be taken in extracting the bare  $d_{x^2-y^2}$  band, far below the Fermi level it anticrosses with several other bands, so the bare dispersion must be chosen to follow the  $d_{x^2-y^2}$  spectral weight.<sup>65</sup>
- <sup>65</sup>P. R. C. Kent, T. Saha-Dasgupta, O. Jepsen, O. K. Andersen, A. Macridin, T. A. Maier, M. Jarrell, and T. C. Schulthess, *Phys. Rev. B* **78**, 035132 (2008).
- <sup>66</sup>W. Zhang, G. Liu, J. Meng, L. Zhao, H. Liu, X. Dong, W. Lu, J. S. Wen, Z. J. Xu, G. D. Gu, T. Sasagawa, G. Wang, Y. Zhu, H. Zhang, Y. Zhou, X. Wang, Z. Zhao, C. Chen, Z. Xu, and X. J. Zhou, *Phys. Rev. Lett.* **101**, 017002 (2008).
- <sup>67</sup>Q. Wang, Z. Sun, E. Rotenberg, H. Berger, H. Eisaki, Y. Aiura, and D. S. Dessau, [arXiv:0910.2787](#).

- <sup>68</sup>R. Löwenich, A. B. Schumacher, J. S. Dodge, D. S. Chemla, and L. L. Miller, *Phys. Rev. B* **63**, 235104 (2001).
- <sup>69</sup>F. Marsiglio and J. P. Carbotte, *Phys. Rev. B* **36**, 3937 (1987).
- <sup>70</sup>J. P. Carbotte, *Rev. Mod. Phys.* **62**, 1027 (1990).
- <sup>71</sup>T. Dahm, V. Hinkov, S. V. Borisenko, A. A. Kordyuk, V. B. Zabolotnyy, J. Fink, B. Bchner, D. J. Scalapino, W. Hanke, and B. Keimer, *Nat. Phys.* **5**, 217 (2009).
- <sup>72</sup>J. G. Storey, J. L. Tallon, and G. V. M. Williams, *Phys. Rev. B* **76**, 174522 (2007).
- <sup>73</sup>A. Kopp, A. Ghosal, and S. Chakravarty, *Proc. Natl. Acad. Sci. USA* **104**, 6123 (2007).
- <sup>74</sup>M. L. Cohen and P. W. Anderson, in *Superconductivity in d- and f-Band Metals*, edited by D. H. Douglass (American Institute of Physics, New York, 1972), p. 17.
- <sup>75</sup>L. F. Tocchio, F. Becca, A. Parola, and S. Sorella, *Phys. Rev. B* **78**, 041101(R) (2008); F. Becca, L. F. Tocchio, and S. Sorella, *J. Phys.: Conf. Ser.* **145**, 012016 (2009).
- <sup>76</sup>R. S. Markiewicz, J. Lorenzana, and G. Seibold, *Phys. Rev. B* **81**, 014510 (2010).
- <sup>77</sup>H. Eskes, M. B. J. Meinders, and G. A. Sawatzky, *Phys. Rev. Lett.* **67**, 1035 (1991).
- <sup>78</sup>R. S. Markiewicz, Tanmoy Das, and A. Bansil, *Phys. Rev. B* **82**, 224501 (2010).
- <sup>79</sup>J. R. Schrieffer, X. G. Wen, and S. C. Zhang, *Phys. Rev. B* **39**, 11663 (1989).
- <sup>80</sup>G. Vignale and M. R. Hedayati, *Phys. Rev. B* **42**, 786 (1990).
- <sup>81</sup>R. S. Markiewicz, T. Das, S. Basak, and A. Bansil, *J. Elect. Spect. Rel. Phenom.* **181**, 23 (2010).
- <sup>82</sup>Tanmoy Das, Ph.D. thesis, Northeastern University.
- <sup>83</sup>R. S. Markiewicz, S. Sahrakorpi, M. Lindroos, Hsin Lin, and A. Bansil, *Phys. Rev. B* **72**, 054519 (2005).
- <sup>84</sup>The band structure is taken to be doping independent in the spirit of the rigid band model,<sup>85</sup> which is expected to be a good approximation for doping away from the CuO<sub>2</sub> planes. It will be interesting to examine doping effects via first-principles approaches.<sup>86</sup>
- <sup>85</sup>A. Bansil, *Phys. Rev. B* **20**, 4025 (1979); **20**, 4035 (1979); R. Prasad and A. Bansil, *ibid.* **21**, 496 (1980); H. Asonen, M. Lindroos, M. Pessa, R. Prasad, R. S. Rao, and A. Bansil, *ibid.* **25**, 7075 (1982).
- <sup>86</sup>S. N. Khanna, A. K. Ibrahim, S. W. McKnight, and A. Bansil, *Solid State Commun.* **55**, 223 (1985); L. Huisman, D. Nicholson, L. Schwartz, and A. Bansil, *Phys. Rev. B* **24**, 1824 (1981); L. Schwartz and A. Bansil, *ibid.* **10**, 3261 (1974).
- <sup>87</sup>G. D. Mahan, *Many-Particle Physics*, 2nd ed. (Plenum, New York, 1990).
- <sup>88</sup>S. G. Sharapov and J. P. Carbotte, *Phys. Rev. B* **72**, 134506 (2005).
- <sup>89</sup>J. Hwang, *Phys. Rev. B* **83**, 014507 (2011).